STEM CELLS AND DEVELOPMENT
Volume 22, Number 16, 2013

DOI: 10.1089/scd.2012.0647

Role of Pericytes in Skeletal Muscle Regeneration and Fat Accumulation

Alexander Birbrair,[1,2] Tan Zhang,[1] Zhong-Min Wang,[1] Maria Laura Messi,[1] Grigori N. Enikolopov,[3,4] Akiva Mintz,[5] and Osvaldo Delbono[1,2]

Stem cells ensure tissue regeneration, while overgrowth of adipogenic cells may compromise organ recovery and impair function. In myopathies and muscle atrophy associated with aging, fat accumulation increases dysfunction, and after chronic injury, the process of fatty degeneration, in which muscle is replaced by white adipocytes, further compromises tissue function and environment. Some studies suggest that pericytes may contribute to muscle regeneration as well as fat formation. This work reports the presence of two pericyte subpopulations in the skeletal muscle and characterizes their specific roles. Skeletal muscle from Nestin-GFP/NG2-DsRed mice show two types of pericytes, Nestin-GFP-/NG2-DsRed+ (type-1) and Nestin-GFP+/NG2-DsRed+ (type-2), in close proximity to endothelial cells. We also found that both Nestin-GFP-/NG2-DsRed+ and Nestin-GFP+/NG2-DsRed+ cells colocalize with staining of two pericyte markers, PDGFRβ and CD146, but only type-1 pericyte express the adipogenic progenitor marker PDGFRα. Type-2 pericytes participate in muscle regeneration, while type-1 contribute to fat accumulation. Transplantation studies indicate that type-1 pericytes do not form muscle in vivo, but contribute to fat deposition in the skeletal muscle, while type-2 pericytes contribute only to the new muscle formation after injury, but not to the fat accumulation. Our results suggest that type-1 and type-2 pericytes contribute to successful muscle regeneration which results from a balance of myogenic and nonmyogenic cells activation.

Introduction

Ectopic adipocyte deposition in the skeletal muscle characterizes various disorders, including obesity/type-2 diabetes, sarcopenia, and muscular dystrophies [1–4]. Progressive fat accumulation resulting in muscle weakness and atrophy [5,6] is a measure of the severity of Duchenne muscular dystrophy (DMD) [7].

Shefer and coworkers once suggested that, in skeletal muscle, adipogenic cells originate from satellite cells through an alternative lineage dictated by a pathological environment [8]. They demonstrated that myogenic and adipogenic cells are associated with the same myofiber in culture but not that fat and muscle arise from the same cell. In a more recent study, Starkey and colleagues conclude that skeletal muscle satellite cells are committed solely to myogenesis [9].

Another group reports that skeletal muscle resident cells expressing PDGFRα contribute to ectopic fat formation in skeletal muscle [10]; are distinct from myogenic progenitors in undamaged young adult muscle; and cannot be recruited to a myogenic lineage in vitro or in vivo [10].

Although satellite cells are generally accepted as a major source of progenitors for adult muscle regeneration, other cells have been shown to have myogenic capacity. During the postnatal period, skeletal muscle pericytes contribute to muscle growth and the satellite cell pool [11–13], and when cultured under appropriate conditions, they differentiate into multilocular adipocytes [13].

We recently identified two *bona fide* pericyte subtypes, type-1 (Nestin−/NG2+) and type-2 (Nestin+/NG2+), in the skeletal muscle interstitium. These cells express the pericyte markers NG2, PDGFRβ, and CD146 and are associated with capillaries. We found that type-2 but not type-1 form neural cells when exposed to optimized media conditions [14,15]. However, whether these pericyte subtypes can differentiate into various mesodermal lineages is unknown.

The fact that PDGFRα-expressing adipogenic cells do not differentiate into the myogenic lineage [10] and that adipogenic and myogenic pericytes are present in skeletal muscle [13] suggests that adipose tissue accumulation might result from the PDGFRα+ nonmyogenic pericyte subtype and skeletal muscle from PDGFRα- myogenic pericytes. Whether

Departments of [1]Internal Medicine-Gerontology, [2]Neuroscience Program, and [5]Neurosurgery, Wake Forest School of Medicine, Winston-Salem, North Carolina.
[3]Cold Spring Harbor Laboratory, Cold Spring Harbor, New York.
[4]NBIC, Moscow Institute of Physics and Technology, Moscow, Russia.

these pericyte subpopulations correspond to the subtypes we have described [16] remains unclear. To examine this hypothesis, we performed flow cytometric analysis in cells derived from skeletal muscle and found that PDGFRα is expressed in Nestin−/NG2+ type-1 pericytes. Further, in vitro experiments show that type-1 pericytes differentiate into adipocytes but not myogenic cells. In contrast, Nestin+/NG2+ type-2 pericytes do not express PDGFRα or differentiate into adipocytes but form myotubes in culture.

Here for the first time, we demonstrate in vivo that after injury, type-1 pericytes do not form muscle but contribute to fat infiltration, while type-2 pericytes form muscle but not fat. These findings suggest that type-1 pericytes contribute to fat accumulation in the skeletal muscle in pathological entities characterized by muscle degeneration/regeneration and extensive fat infiltration.

Materials and Methods

Animals

Our colony of Nestin-GFP transgenic mice was maintained homozygous for the transgene on the C57BL/6 genetic background [17]. Our colony of C57BL/6 wild-type mice was used as the control. Male athymic nude (nu/nu) mice from Taconic Farms were used in transplantation studies. NG2-DsRed transgenic mice expressing DsRed-T1 under the control of the NG2 promoter [18] and β-actin-DsRed transgenic mice expressing red fluorescent protein variant DsRed.MST under the control of the chicken β-actin promoter coupled with the cytomegalovirus immediate-early enhancer [19] were purchased from the Jackson Laboratory.

All tissues of β-actin-DsRed transgenic mice fluorescence red [19]. Nestin-GFP mice were crossbred with (1) NG2-DsRed mice to generate Nestin-GFP/NG2-DsRed double-transgenic mice; and (2) β-actin-DsRed mice to generate Nestin-GFP/β-actin-DsRed double-transgenic mice.

All colonies were housed in a pathogen-free facility of the Animal Research Program at Wake Forest School of Medicine (WFSM) under a 12:12-h light/dark cycle and fed *ad libitum*. Both male and female homozygous mice were used, and their ages ranged from 3 to 5 months. The WFSM Animal Care and Use Committee approved handling and procedures.

Fluorescence-activated cell sorting

Fluorescence-activated cell sorting (FACS) was carried out on a BD FACS (Aria Sorter) at 4°C and a pressure of 20 psi, using a laser at the 488-nm line, a 530/30 band-pass filter, a 100-μm sorting tip, and 34.2 kHz drive frequency. The sorting apparatus was sterilized with 10% bleach. This instrument allowed us to characterize cells by size as well as fluorescence. Data acquisition and analyses were performed using BD FACS Diva 5.0.3 software, gated for a high level of GFP, DsRed, or APC expression. The clear separation of GFP+ from GFP− cells [14] and DsRed+ from DsRed− cells as well as the low flow rate explains the ease and accuracy of sorting [16]. Sorted cells were reanalyzed to confirm their fluorescence profile [14,16].

Primary antibodies

Table 1 shows antibodies, their dilution, and source.

PDGFRα analysis by flow cytometry

Fresh cells were dissociated from the skeletal muscle of Nestin-GFP/NG2-DsRed mice as described [14–16] and processed for immunofluorescence staining as described [15]. For analysis, 10^5 cells were incubated with PDGFRα primary rabbit anti-mouse antibody, kindly provided by Dr. W. Stallcup (Sanford-Burnham Medical Research Institute). First, an aliquot was collected for use as unlabeled control (labeled with only the secondary APC anti-rabbit, without the primary anti-PDGFRα antibody). The remainder were incubated with the primary PDGFRα antibody for 45 min and washed in phosphate buffered saline (PBS) with 1% fetal bovine serum (FBS). They were then incubated for 30 min with APC anti-rabbit secondary antibody, washed in PBS with 1% FBS, and run on a BD FACS flow cytometer (Aria Sorter).

Table 1. Antibodies, Concentration, and Source

Antibody	*Dilution*	*Source*	*Location*
Rat anti-CD31 (PECAM-1)	1:100	BD Biosciences	San Jose, CA
Rat anti-mouse CD146	1:250	BioLegend	San Diego, CA
Rabbit anti-PDGFRβ	1:250	Dr. W. Stallcup	Sanford-Burnham Medical Research Institute, CA
Rabbit anti-PDGFRα	1:250	Dr. W. Stallcup	Sanford-Burnham Medical Research Institute, CA
Rabbit anti-Perilipin A	1:250	Sigma	St. Louis, MO
Mouse anti-Myogenin (F5D)	1:400	Developmental Studies Hybridoma Bank, University of Iowa	Iowa City, IA
Mouse anti-MHC (MF 20)	1:2,000	Developmental Studies Hybridoma Bank, University of Iowa	Iowa City, IA
Rabbit anti-Laminin	1:250	Sigma	St. Louis, MO
Rabbit anti-NG2 Chondroitin sulfate proteoglycan	1:100	Chemicon-Millipore	Temecula, CA
Mouse anti-Pax7	1:100	Developmental Studies Hybridoma Bank, University of Iowa	Iowa City, IA
Rat anti-Ki67	1:100	DakoCytomation	Carpinteria, CA

Immunohistochemistry

To detect DsRed and GFP fluorescence, *tibialis anterior* (TA) muscles from 3-month-old Nestin-GFP/NG2-DsRed mice or nude mice injected with DsRed+ pericytes were dissected; fixed in 4% paraformaldehyde (PFA) overnight; immersed in 10%, 20%, and 30% sucrose solutions for 60, 45, and 30 min, respectively; embedded in optimal cutting temperature (OCT); and rapidly frozen in liquid nitrogen to prepare 10-μm-thick cryosections. Muscle sections were fixed with 4% PFA for 30 min, then permeabilized in 0.5% Triton X-100 (Sigma), and blocked to saturate nonspecific antigen sites using 5% (v/v) goat serum/PBS (Jackson Immunoresearch Labs) overnight at 4°C. The next day, the sections were incubated with primary antibodies at room temperature for 4 h and visualized using appropriate species-specific secondary antibodies conjugated with Alexa Fluor 488, 568, 647, or 680 at 1:1,000 dilution (Invitrogen). Muscle sections were counterstained with Hoechst 33342, mounted on slides using Fluorescent Mounting Medium (DakoCytomation), and examined under fluorescence microscopy.

Cell isolation from Nestin-GFP/NG2-DsRed mice skeletal muscle by FACS

A pool of hindlimb muscles was used in experiments to induce adipogenic and myogenic cells in vitro. Fresh cells were sorted immediately after their dissociation from skeletal muscle. Hindlimb muscles from young-adult (3–5-month-old) Nestin-GFP/NG2-DsRed transgenic mice were prepared as described [14–16]. Briefly, muscles were carefully dissected away from the surrounding connective tissue and minced, then digested by gentle agitation in 0.2% (w/v) type-2 collagenase in Krebs solution at 37°C for 2 h, and dissociated by trituration and resuspension in 0.25% trypsin/0.05% ethylenediaminetetraacetic acid (EDTA) in PBS for 15 min at 37°C. After centrifuging at 1,500 rpm for 5 min, the supernatant was removed, and the pellet resuspended in growth medium. Aggregates were removed by passing them through a 40-μm cell strainer before sorting. Cells were centrifuged at 1,500 rpm for 5 min. The supernatant was removed, and the pellet resuspended in 1% FBS in PBS, and analyzed for GFP and DsRed fluorescence to sort the different cell populations based on these two markers. The gate was set using cells isolated from C57BL6 wild-type mice. Isolated Nestin-GFP−/NG2-DsRed+ and Nestin-GFP+/NG2-DsRed+ cells were cultured in conditions conducive to either adipocyte or myocyte induction, and morphology, Oil Red O staining, and perilipin, myogenin, and myosin heavy chain (MHC) expression were analyzed.

Adipogenic induction in vitro

Adipogenic differentiation was induced in adipogenic medium for 14 days as described [13]. Briefly, freshly isolated pericyte subtypes were plated onto laminin-coated plates (Invitrogen) in Dulbecco's modified Eagle medium (DMEM) supplemented with 10% FBS (Invitrogen), 1 μM dexamethasone (Sigma), 0.5 μM isobutylmethylxanthine (Fisher Scientific), 60 μM indomethacine (Sigma), and 170 μM insulin (Invitrogen), and maintained in a 5% CO_2 atmosphere. After 14 days, cells were fixed in 4% PFA at room temperature (RT), followed by Oil Red O and perilipin staining for lipid detection.

Oil Red O and hematoxylin staining

To qualitatively examine adipogenesis, lipid accumulation was analyzed by staining cells with the lipid-specific dye Oil Red O, which stains cytoplasmic lipid deposits red, as described [20]. Briefly, cells cultured in petri dishes for 14 days were fixed in 4% PFA, washed with 60% isopropanol, allowed to dry completely, submerged in a 0.5% filtered solution of Oil Red O in propylene glycol, and washed in graded propylene glycol solutions. They were then washed many times, counterstained with Harris hematoxylin, and washed again. Analysis was performed using bright field microscopy.

Myogenic induction in vitro

Freshly isolated pericyte subtypes (2×10^3 cells per cm^2) were cultured on laminin-precoated plates (Invitrogen) for 3 days in growth medium [DMEM-high glucose (Invitrogen), supplemented with 2% L-glutamine, 50 U/mL penicillin, 50 mg/mL streptomycin, and 10% (v/v) FBS (Invitrogen)]. Myogenic differentiation was induced by lowering serum concentration to 2%, using differentiation medium [DMEM (Invitrogen) containing 2-mM L-glutamine (Invitrogen) and 1% penicillin/streptomycin (Invitrogen), supplemented with 2% Horse Serum (Invitrogen)] for an additional 14 days in a 5% CO_2 atmosphere. Medium was changed every 4 days until elongated, multinucleated myofibers appeared. After day 3 and day 14, cells were fixed in 4% PFA at RT, and myogenin and MHC expression were quantified.

Immunocytochemistry

Cultured cells were fixed with 4% PFA for 30 min, then permeabilized in 0.5% Triton X-100 (Sigma), and blocked to saturate nonspecific antigen sites using 5% (v/v) goat serum/PBS (Jackson Immunoresearch Labs) overnight at 4°C. The next day, the cells were incubated with primary antibodies at room temperature for 4 h and visualized using appropriate species-specific secondary antibodies conjugated with Alexa Fluor 488, 568, 647, or 680 at 1:1,000 dilution (Invitrogen). They were counterstained with Hoechst 33342 reagent at 1:2,000 dilution (Invitrogen) to label the DNA and mounted on slides for fluorescent microscopy with Fluorescent Mounting Medium (DakoCytomation).

Flexor digitorum brevis muscle single-fiber dissociation

Flexor digitorum brevis (FDB) muscles from Nestin-GFP/NG2-DsRed transgenic mice were used to analyze the Nestin-GFP+ cells attached to the myofibers. FDB muscle was preferred over more traditional muscles for this experiment because it is small and flat, allowing more complete dissociation by trituration in a single step and shortening the experiment significantly [21,22]. Methods for FDB muscle dissociation have been described [14–16]. Briefly, muscles were carefully dissected away from the surrounding connective tissue and minced, then digested by gentle agitation in 0.2% (w/v) Worthington's type-2 collagenase in Krebs solution at 37°C for 2 h. They were resuspended in growth medium and dissociated by gentle trituration. The growth medium consisted of DMEM-high glucose (Invitrogen),

supplemented with 2% L-glutamine, 50 U/mL penicillin, 50 mg/mL streptomycin, and 10% (v/v) FBS (Invitrogen). After dissociation, Nestin-GFP+/NG2-DsRed+ and Nestin-GFP+/NG2-DsRed− cells attached to myofibers were counted.

Reverse transcription polymerase chain reaction

To detect the mRNA expression in cells, total RNA was isolated using TRIZOL reagent (Life Technologies), RNA was dissolved in sterile, RNase-free water (Invitrogen) and quantitated spectrophotometrically at 260 nm. Reverse transcription polymerase chain reaction (RT-PCR) was performed in accordance with the manufacturer's instructions using the SuperScript III First-Strand synthesis system for RT-PCR system (Invitrogen). For each experiment, equivalent amounts of intact RNA (0.1–0.2 μg) were used. As negative controls, the RT reactions were performed in the absence of RNA (only water) or reverse transcriptase. The cDNA was amplified by PCR using the primers included in Table 2. PCR Master Mix was purchased from Promega. Each PCR contained 1× Promega PCR Master Mix, 1 μM of each primer, and the cDNA of the cell used in each case (Nestin-GFP+/NG2-DsRed−, Nestin-GFP−/NG2-DsRed+, or Nestin-GFP+/NG2-DsRed+ cell). The volume of each reaction was brought up to 50 μL with water. DNA amplification was carried out as follows: denaturation at 94°C for 2 min, followed by 35 cycles of 94°C for 1 min, 60°C for 1 min, and 72°C for 2 min. After 35 cycles, the reactions were incubated at 72°C for 7 min to increase the yield of amplification. PCR products were verified with DNA 2% agarose gel electrophoresis.

Isolation of type-1 and type-2 DsRed+ pericytes

Hindlimb muscle cells were isolated from young adult (3–5-month-old) Nestin-GFP/β-actin-DsRed mice as described above [15]. After counting, cells were centrifuged at 1,500 rpm for 5 min and resuspended in 100 μL 1% FBS in PBS per 10^6 cells. An aliquot was collected for use as unlabeled control, while the remaining cells were labeled with APC anti-mouse NG2 antibody for 45 min. After washing, they were resuspended in 1% FBS in PBS and sorted using GFP and APC fluorescence. Isolated Nestin-GFP+/NG2-APC+/β-actin-DsRed+ and Nestin-GFP−/NG2-APC+/β-actin-DsRed+ cells were used in cell fate tracking experiments to evaluate adipogenesis and myogenesis in vivo.

Muscle injury and cell transplantation

Skeletal muscle regeneration was studied in TA muscle injured by intramuscular injection of barium chloride ($BaCl_2$) as described [23,24]. Specifically, immunodeficient, 3–5-month-old mice were anaesthetized by isoflurane/O_2 inhalation. TA muscles were injected with 50 μL of 1.2% $BaCl_2$ dissolved in sterile PBS one day before cell transplantation. At 24 h postinjury, type-1 (Nestin-GFP−/NG2-APC+/β-actin-DsRed+) or type-2 (Nestin-GFP+/NG2-APC+/β-actin-DsRed+) pericytes were isolated from donor Nestin-GFP/β-actin-DsRed mice, resuspended in PBS (1.5×10^4 cells per TA), and slowly injected into the damaged muscle of the acceptor mice. As a control, injured TA muscles were injected with PBS. Mice were sacrificed 14 days postinjection, and TA muscles collected and processed for immunohistochemistry as described above. The number of newly formed DsRed+ myofibers with central nuclei was quantified in the muscle sections.

Skeletal muscle fatty degeneration and cell transplantation

For in vivo adipogenic analysis, skeletal muscle fatty degeneration was induced as described [10,25,26]. Briefly, 1 day before the sorted pericyte populations (3×10^4 cells in 30 μL PBS) were implanted, the TA muscles of immunodeficient wild-type mice were injected with a 29-gauge needle containing 100 μL of 50% v/v glycerol. Two weeks later, the mice were sacrificed, and their TA muscles immediately excised and processed for immunohistochemistry as described [16]. DsRed+ cells positive to perilipin A, which is localized at the adipocyte's lipid droplet surface [27], were counted in muscle sections.

Microscopy, cell imaging, and counting

An inverted motorized fluorescent microscope (Olympus IX81) with an Orca-R2 Hamamatsu charge-coupled device (CCD) camera was used for image acquisition. Camera drive and acquisition were controlled by a MetaMorph Imaging System (Olympus). Ten arbitrary microscopic fields were counted in each immunostained plate or each slide, and values pooled from parallel triplicates per timepoint and individual experiment.

Statistical analysis

Results are expressed as the mean ± standard error of the mean (SEM). Statistical significance was assessed by Student's

Table 2. Genes, GenBank Accession Numbers, Coding Regions, Primers

Gene	*GenBank accession numbers*	*Coding regions*	*Forward primer and positions*	*Reverse primer and positions*
Myf5	NM_008656.5	CDS: 204–971	AGACGCCTGAAGAAGGTCAA (483–502)	TGGAGAGAGGGAAGCTGTGT (899–880)
CD34	NM_001111059.1	CDS: 146–1123	GGGTAGCTCTCTGCCTGATG (195–214)	CAGTTGGGGAAGTCTGTGGT (482–463)
Sca-1	NM_010738.2	CDS: 39–443	CCATCAATTACCTGCCCCTA (162–181)	AAGGTCTGCAGGAGGACTGA (436–417)
Pax7	NM_011039.2	CDS: 58–1569	CATCCTTAGCAACCCGAGTG (1215–1234)	AGTAGGCTTGTCCCGTTTCC (1567–1548)
GAPDH	NM_008084.2	CDS: 51–1052	GTGGCAAAGTGGAGATTGTTGCC (118–140)	GATGATGACCCTTTTGGCTCC (407–387)

t-test using GraphPad Prism (GraphPad Software). $P < 0.05$ was considered significant.

Results

Two bona fide pericyte subpopulations in skeletal muscle

Pericyte heterogeneity has been described in spinal cord scar tissue by Goritz et al. [28] and in skeletal muscle by our group [16]. Skeletal muscle histological sections from Nestin-GFP/NG2-DsRed mice support our previous results in cultured cells, showing two types of pericytes, Nestin-GFP−/NG2-DsRed+ and Nestin-GFP+/NG2-DsRed+, in close proximity to endothelial cells and surrounding capillaries labeled with CD31, a endothelial cell marker [29] (Fig. 1A). We also found that both Nestin-GFP−/NG2-DsRed+ and Nestin-GFP+/NG2-DsRed+ cells colocalize with staining of two pericyte markers, PDGFRβ [30] and CD146 [13,31] (Fig. 1B).

Pericytes may act as myogenic [11–13] or adipogenic progenitors [13,32]. As myogenic potential was not reported in adipogenic progenitors [10], here we hypothesize that the two pericyte subtypes differ, and one contributes to the skeletal muscle fat accumulation observed in fatty degeneration in the muscle [10], while the other to myogenesis under normal conditions [11,13,33].

Type-1 but not type-2 pericytes express the adipogenic progenitor marker PDGFRα

To elucidate whether one of the muscle pericyte subpopulations, we described [16] is a adipogenic progenitor [10,25], we performed flow cytometry analysis based on the adipogenic progenitor marker PDGFRα [10,25] in mononucleated cells from Nestin-GFP/NG2-DsRed mouse skeletal muscle. We found that PDGFRα is expressed in a fraction of the two cell populations, Nestin-GFP−/NG2-DsRed- and Nestin-GFP−/NG2-DsRed+ cells (Fig. 2A, B). Note that type-1 pericytes expressed PDGFRα, while type-2 pericytes did not. We confirmed our results in skeletal muscle in vivo (Fig. 2C).

Type-1 but not type-2 pericytes are adipogenic in vitro

To evaluate whether in addition to expressing the adipogenic progenitor marker, type-1 pericytes have adipogenic potential, we isolated type-1 and type-2 pericytes using Nestin-GFP/NG2-DsRed mice and cultured them separately in adipogenic induction medium (Fig. 3A, B). We used Oil Red O, which stains neutral triglycerides and lipids, and immunocytochemistry to look for the expression of perilipin, an essential protein for lipid storage and lipolysis [27] located exclusively on adipocyte lipid droplets [34]. Consistent with our results on PDGFRα expression, only type-1 pericytes differentiated into adipocytes in culture. The percentage of perilipin+ cells/nuclei derived from type-1 and type-2 pericyte cultures was 37%±8.2% and 0.16%±0.10%, respectively (Fig. 3C, D), and the percentage of Oil Red O+ cells/nuclei was 38%±2.8% and 0.29%±0.18% cells, respectively (Fig. 3E, F). Supplementary Figure S1 (Supplementary Data are available online at www.liebertpub.com/scd) shows that a subpopulation of PDGFRα+ type-1 pericytes forms adipocytes in vitro, consistently with the adipogenic potential reported for

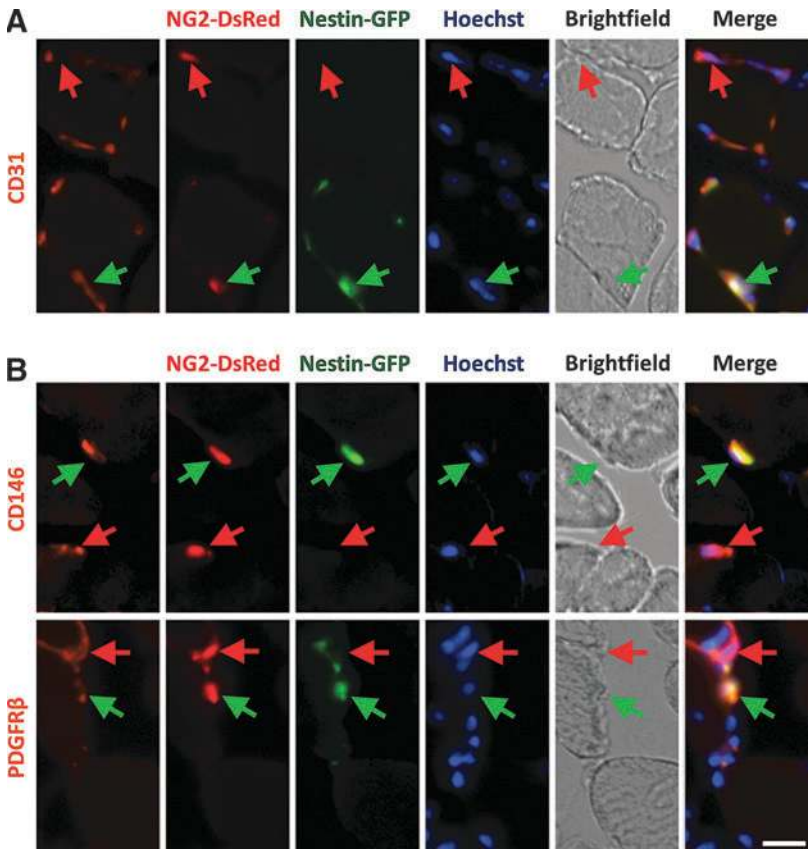

FIG. 1. Two bona fide pericyte subtypes in skeletal muscle. Histological analysis of pericyte subtypes in the skeletal muscle from Nestin-GFP/NG2-DsRed mice. **(A)** Pericytes surround the endothelial cell layers of the capillary network in skeletal muscle. Muscle section showing small blood vessels with CD31+ endothelial cells, characteristically surrounded by NG2-DsRed+ pericytes. Nestin-GFP−/NG2-DsRed+ (type-1) (*red arrow*) and Nestin-GFP+/NG2-DsRed+ (type-2) (*green arrow*) pericytes and the blood vessels' CD31+ (*orange*) labeled contour. All *panels* show the same area for different channels (Nestin-GFP, NG2-DsRed, Hoechst, CD31 staining, brightfield, merged fluorescence images, and all the images merged with brightfield). **(B)** Pericyte markers PDGFRβ and CD146 colocalize with skeletal muscle interstitial Nestin-GFP−/NG2-DsRed+ and Nestin-GFP+/NG2-DsRed+ cells. The *top* and *bottom* six *panels* show identical muscle areas from *left* to *right*: CD146 (*top*) or PDGFRβ (*bottom*) (*orange*), NG2-DsRed (*red*), Nestin-GFP+ (*green*), Hoechst (*blue*), brightfield, and merged images. The *red arrow* indicates type-1 pericytes (Nestin-GFP−/NG2-DsRed+ cells), and the *green arrow*, type-2 (Nestin-GFP+/NG2-DsRed+ cells). Scale bar = 20 μm. Color images available online at www.liebertpub.com/scd

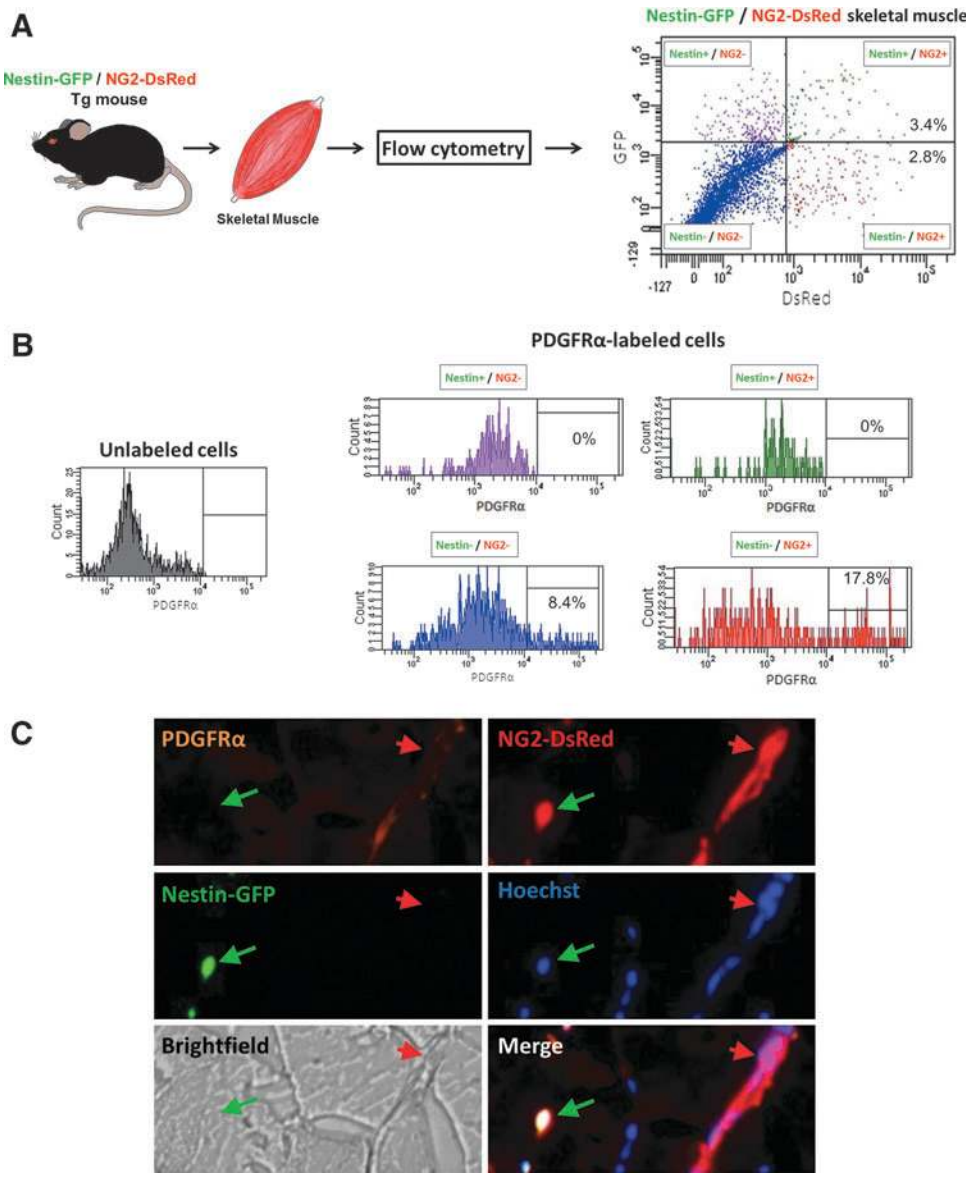

FIG. 2. PDGFRα expression in a subpopulation of type-1 but not type-2 pericytes. **(A)** Isolation of skeletal muscle cells for flow cytometry. Representative dot plot showing GFP versus DsRed fluorescence with the gate set using cells isolated from wild-type mice. The cells were divided into four populations: Nestin-GFP + /NG2-DsRed – (*purple*), Nestin-GFP – /NG2-DsRed + (*red*), Nestin-GFP + /NG2-DsRed + (*green*), and Nestin-GFP – /NG2-DsRed – (*blue*). **(B)** Flow cytometry analysis of PDGFRα expressed by skeletal muscle-derived cells. Histograms show PDGFRα expression in each population. *Left* histogram (unlabeled cells) shows control staining of all cells with secondary antibody APC anti-rabbit to set the gate without using primary antibody rabbit anti-PDGFRα. *Right* histograms (PDGFRα-labeled cells) show the surface expression of PDGFRα on each skeletal muscle-derived cell subset. Data represent three independent experiments in cells dissociated from the hindlimb muscles of Nestin-GFP/NG2-DsRed mice. Note that only Nestin-GFP – /NG2-DsRed – and Nestin-GFP – /NG2-DsRed + cells express PDGFRα. **(C)** Representative transverse cross-section of a tibialis anterior muscle from a double-transgenic Nestin-GFP/NG2-DsRed mouse. A *green arrow* indicates a Nestin-GFP + /NG2-DsRed + cell, and a *red arrow*, a Nestin-GFP – /NG2-DsRed + cell. Expression of PDGFRα, GFP, DsRed, and their corresponding, Hoechst 33342, brightfield, and merge images are illustrated. PDGFRα staining colocalizes with skeletal muscle interstitial Nestin-GFP – /NG2-DsRed + but not Nestin-GFP + /NG2-DsRed + cells. Color images available online at www.liebertpub.com/scd

muscle-derived PDGFRα + cells [10]. Supplementary Figure S2 shows that type-1 pericytes express Sca-1 and CD34.

Type-2 but not type-1 pericytes differentiate into muscle cells in vitro

To examine whether adipogenic progenitors form muscle cells [10], we evaluated the myogenic potential of the two skeletal muscle pericyte subpopulations (Fig. 4A, B). As pericytes differentiated into myofibers [11,13], we exposed them to myogenic differentiation conditions and examined the expression of myogenin, a marker of cell differentiation [35], and MHC, a myotube marker [36]. We found that only type-2 pericytes differentiated into the muscle lineage (Fig. 4). The percent of myogenin + cells/nuclei derived from type-1 and type-2 pericytes was 0.18% ± 0.18% and

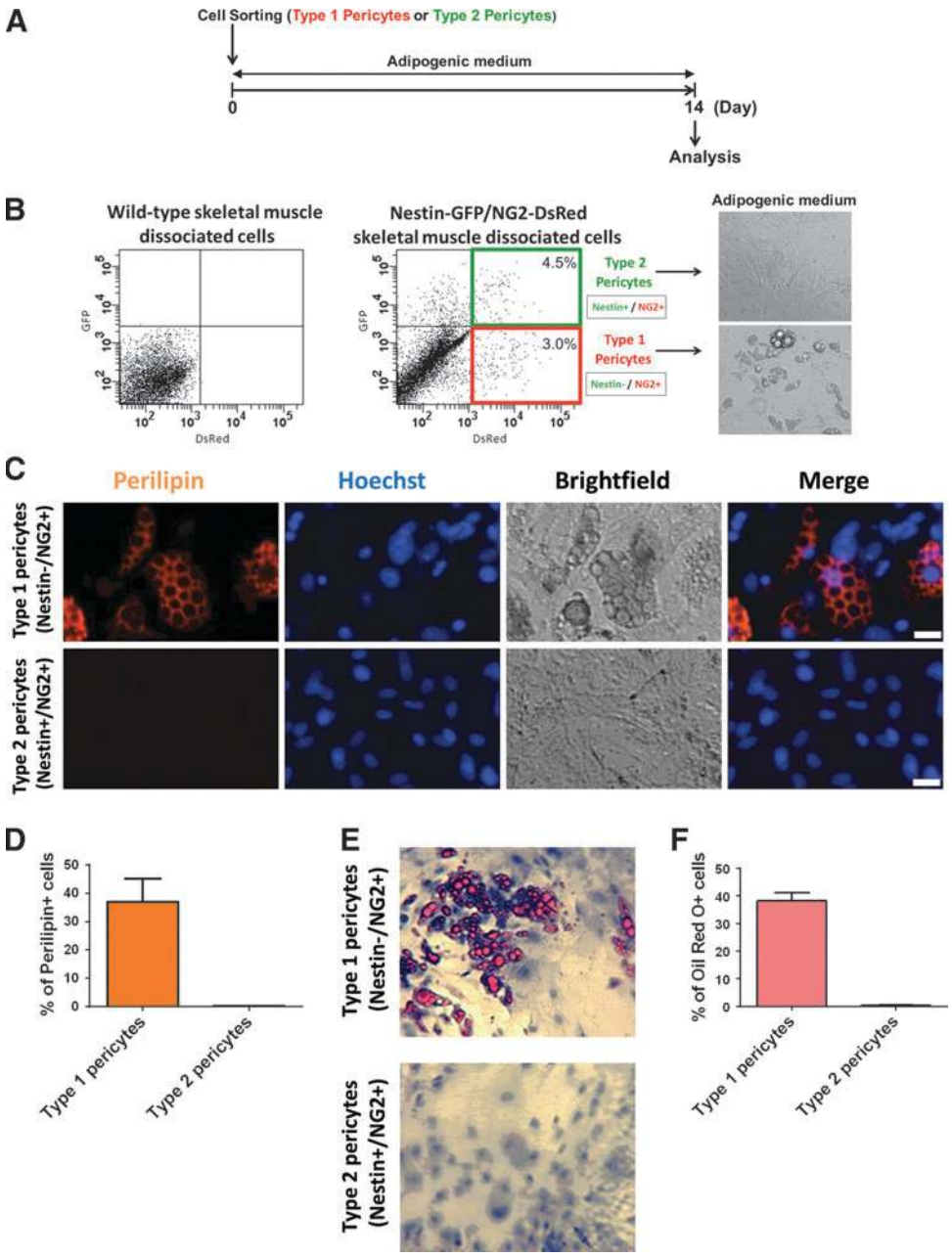

FIG. 3. Type-1 but not type-2 pericytes are adipogenic in vitro. Adipogenic induction of freshly isolated muscle-derived pericyte subtypes. **(A)** Protocol: freshly isolated pericytes were cultured in adipogenic medium for 14 days. **(B)** Representative dot plots showing DsRed versus GFP fluorescence of cells isolated from skeletal muscle of Nestin-GFP/NG2-DsRed mice. Gate was set using cells derived from wild-type skeletal muscle. Morphologic analysis is shown after type-1 and 2 pericytes were cultured for 2 weeks under adipogenic conditions; they were then stained with anti-perilipin A antibody **(C, D)** or Oil Red O/hematoxylin **(E, F)**. **(D)** Percent of cells positive for perilipin in type-1 or type-2 pericytes ($n=5$ preparations). **(F)** Percent of type-1 or type-2 pericytes positive for Oil Red O ($n=5$ preparations from separate cell isolation experiments). Data are mean ± standard error of the mean (SEM). Scale bars = 20 μm. Color images available online at www.liebertpub.com/scd

12% ± 1.8%, respectively (Fig. 4C, D), and the percentage of MHC+ nuclei/total nuclei was 0.31% ± 0.12% and 55% ± 6.5%, respectively (Fig. 4E, F).

Exclusion of satellite cells as a source of myogenic cells in the Nestin-GFP+/NG2-DsRed+ population

Satellite cells, the oldest known skeletal muscle stem cells committed to myogenesis [37], express GFP in Nestin-GFP transgenic mice [38]. To exclude this potentially confounding factor, we examined whether satellite cells express NG2 proteoglycan, which type-2 pericytes express on their surface.

Satellite cells reside near the myofiber, beneath the basal lamina [37]. We quantified 120 Nestin-GFP+ cells in this location; Nestin-GFP+/NG2-DsRed− cells were sheathed in laminin (basal lamina), but we found no Nestin-GFP+/NG2-DsRed+ cells in the satellite cell niche (Fig. 5A, B). Thus, satellite cells do not express NG2 proteoglycan and differ from type-2 pericytes, which express NG2 and are located outside the basal lamina.

To validate this conclusion, we used a procedure we have previously used [14] to facilitate isolation of intact FDB myofibers with their complete cohort of satellite cells still located beneath the basal lamina. We observed that every cell attached to the myofibers did not express NG2 proteoglycan and detected only Nestin-GFP. However, detached cells, probably derived from the muscle interstitium, expressed NG2, sometimes associated with Nestin-GFP expression, sometimes not, corresponding to type-2 and type-1 pericytes, respectively (Fig. 5C, D). Additionally, the paired box transcription factor Pax7 [39–42] is expressed in satellite cells, but not in NG2-DsRed+ cells (Fig. 5E).

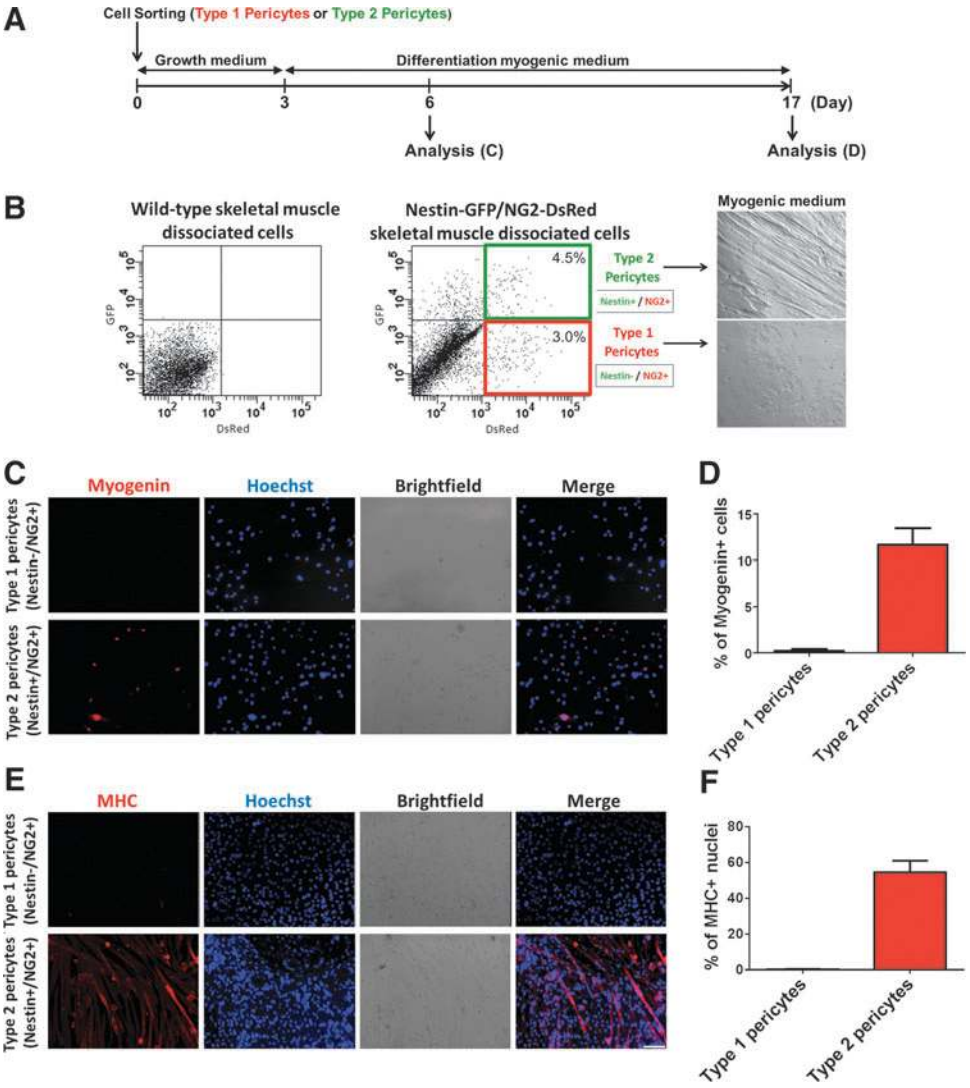

FIG. 4. Type-2 but not type-1 pericytes are myogenic in vitro. Myogenic induction of freshly isolated muscle-derived pericyte subtypes. **(A)** Protocol: freshly isolated pericytes were cultured for 3 days in growth medium followed by 2 weeks in myogenic differentiation medium. **(B)** Representative dot plots showing DsRed versus GFP fluorescence of cells isolated from the skeletal muscle of Nestin-GFP/NG2-DsRed mice. Gate was set using cells derived from wild-type skeletal muscle. Morphologic analysis is shown after type-1 and 2 pericytes were cultured for 2 weeks in myogenic conditions. **(C, D)** After 3 days in differentiation medium, Nestin-GFP − /NG2-DsRed + and Nestin-GFP + /NG2-DsRed + cells were stained with anti-myogenin antibody. **(D)** The percent of myogenin + cells derived from each pericyte population was counted and normalized to the number of nuclei. ($n = 3$ preparations from separate cell isolation experiments). **(E, F)** After 14 days in differentiation medium, both cell types were stained with anti-MHC antibody. **(F)** The percent of MHC + nuclei derived from each pericyte subpopulation was counted and normalized to the total number of nuclei ($n = 3$ preparations from separate cell isolation experiments). Data are mean ± SEM. Scale bar = 100 μm. Color images available online at www.liebertpub.com/scd

As skeletal muscle satellite cells express Myf5 and CD34 [43], but not Sca-1 [44], we examined their expression in Nestin-GFP and NG2-DsRed cells by RT-PCR. Nestin-GFP + / NG2-DsRed − cells and satellite cells exhibit a similar expression profile (Pax7 +, Myf5 +, CD34 +, Sca-1 −), while both pericyte subtypes lack Pax7 and Myf5 markers (Supplementary Fig. S2). These data indicate that the myogenic potential of type-2 pericytes is unrelated to that of satellite cells.

CD34 and Sca-1 expression was detected in type-1 but not type-2 pericytes (Supplementary Fig. S2). A small pericyte subpopulation expresses CD34 [45,46] [47,48] or Sca-1 [49,50]. Here we found that a subpopulation of type-1 pericytes express CD34 and Sca-1 (Supplementary Fig. S2). As PDGFRα + cells have been reported to be CD34 + and Sca-1 + [25], and a subpopulation of them are included in type-1 pericytes (Fig. 2), our data indicate that a subgroup of type-1 pericytes are part of the fibro/adipogenic progenitors cells reported before [25]. Here we also provide initial evidence that type-1 pericytes can be induced to form fibroblasts (Supplementary Fig. S3).

Type-1 and type-2 pericyte subtypes expand after muscle injury

Satellite cells [51] and fibroblasts [52] are activated and proliferate after muscle injury. To assess whether pericytes

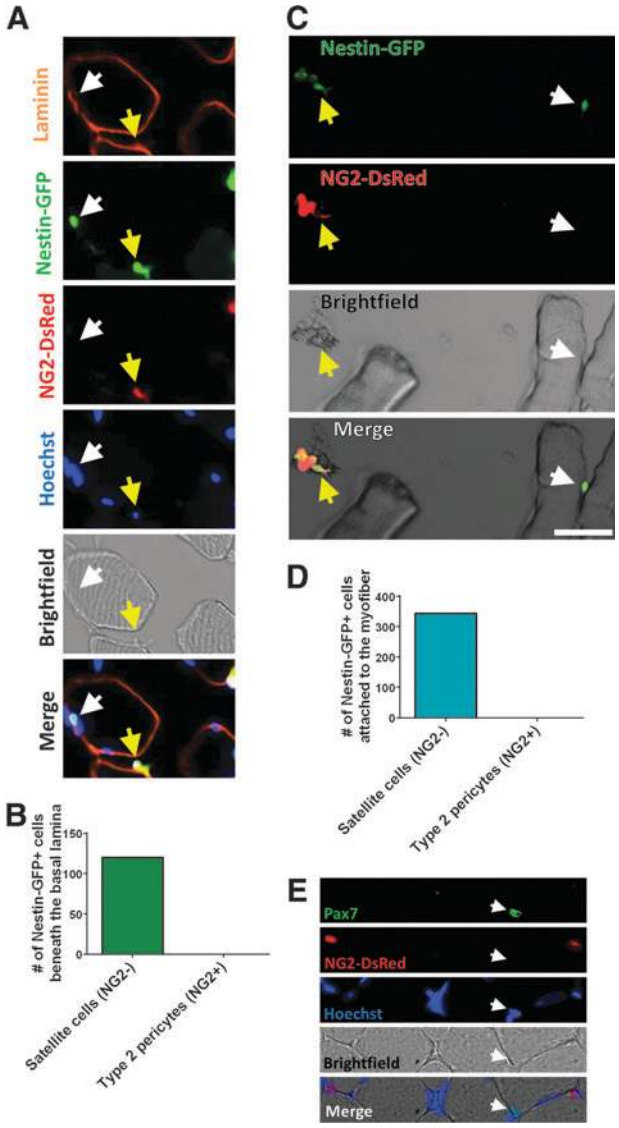

FIG. 5. Satellite cells do not express NG2 proteoglycan. **(A)** Representative tibialis anterior (TA) muscle section from a Nestin-GFP/NG2-DsRed transgenic mouse showing laminin (basal lamina), Nestin-GFP, NG2-DsRed expression, and Hoechst positive nuclei in the same region. Brightfield and merged images are also shown. *White arrow* shows a satellite cell (Nestin-GFP+ located beneath the basal lamina) that does not express NG2-DsRed; the *yellow arrow* indicates a type-2 pericyte (Nestin-GFP+/NG2-DsRed+) located outside the basal lamina. **(B)** We counted 120 Nestin-GFP+ cells (NG2+ or NG2−) beneath the basal lamina. **(C)** Representative Nestin-GFP, NG2-DsRed, brightfield, and merged images of the same region in a dish containing freshly dissociated flexor digitorum brevis (FDB) muscle fibers from Nestin-GFP/NG2-DsRed mice. The *white arrow* indicates a satellite cell (Nestin-GFP+) attached to the myofiber, while the *yellow arrow* shows both types of pericytes (Nestin-GFP−/NG2-DsRed+ and Nestin-GFP+/NG2-DsRed+ cells) in dissociated connective tissue. Scale bar = 50 μm. **(D)** Number of Nestin-GFP+ cells (NG2+ or NG2−) in freshly dissociated single FDB muscle fibers from Nestin-GFP/NG2-DsRed transgenic mice; $n = 4$ preparations, more than 1,000 cells counted. **(E)** Representative TA muscle section from a NG2-DsRed transgenic mouse showing Pax7 staining. The *white arrow* shows a typical satellite cell (Pax7+/NG2-DsRed−). Color images available online at www.liebertpub.com/scd

respond to injury in vivo, we analyzed type-1 and type-2 pericytes in skeletal muscle cross-sections during regeneration (Supplementary Fig. S4). After injury induced with Glycerol or $BaCl_2$, both types of pericytes expand (Supplementary Fig. S4A) and re-enter the cell cycle (Supplementary Fig. S4B, C). We did not detect differences in their response to both types of injury. Similarly to preinjury, a population of PDGFRα+ type-1 pericytes was also detected after injury (Supplementary Fig. S5).

Type-1 but not type-2 pericytes form fat during skeletal muscle fatty degeneration

Given that purified type-1 pericytes have adipogenic differentiation potential in vitro, we next examined their adipogenic capacity in vivo in skeletal muscle.

After chronic injury, muscle is often replaced by white adipocytes that compromise tissue function and environment in a process termed *fatty degeneration* [53]. However, even mouse models of such disorders as DMD or obesity rarely show adipocytes in skeletal muscle. We used a model of muscle fatty degeneration reported in the literature [10,25,26,54–61]. Injecting glycerol in the muscle destabilizes cell membranes, promoting myofiber damage, significant fat deposits along the muscle, and cell death. As in human dystrophy, muscles exhibit extensive ectopic adipocyte infiltration of unknown origin [26]. In the absence of glycerol treatment, intramuscularly injected cells showed no adipocyte differentiation in wild-type young mice (data not shown). We transplanted pericyte subtypes freshly isolated and sorted from muscles of Nestin-GFP/β-actin-DsRed transgenic (Tg) mice. Consistently with a previous publication from our lab [16], the 100% purity of these cells was confirmed by microscopy and flow cytometry (data not shown). Expressing DsRed fluorescence [15], they were injected into the TA muscle of wild-type mice previously injected with glycerol (Fig. 6A, C). At day 14, numerous DsRed+ cells were detected in mice injected with either subtype; however, only mice injected with type-1 pericytes had DsRed+ mature adipocytes with large lipid vacuoles (Fig. 7A). All type-2 pericytes retained their pericyte marker, NG2 proteoglycan, after injection (data not shown).

The adipogenic potential of Nestin-GFP−/NG2+/β-actin-DsRed+ cells was examined further in vivo by immunocytochemistry analysis of perilipin in DsRed+ cells derived from transplanted cells (Fig. 7). Quantitative analysis revealed that adipocytes arose almost exclusively from type-1 pericytes. Nestin-GFP−/NG2+/β-actin-DsRed+ and Nestin-GFP+/NG2+/β-actin-DsRed+ cells formed 260 ± 25 and 4.5 ± 4.5 DsRed+/perilipin+ cells per mm^2, respectively (Fig. 7A, B). These results suggest that type-1 but not type-2 pericytes differentiate into adipocytes in vivo.

Type-2 pericytes are myogenically competent and participate in skeletal muscle regeneration in vivo

Since pericytes exhibit myogenic potential in vivo [11,13], we used a muscle injury model induced by $BaCl_2$ injection, where muscle degeneration is confined and does not damage the basement membrane [62] (Fig. 6A, B).

We transplanted cells isolated from muscles of Nestin-GFP/β-actin-DsRed transgenic (Tg) mice into the TA

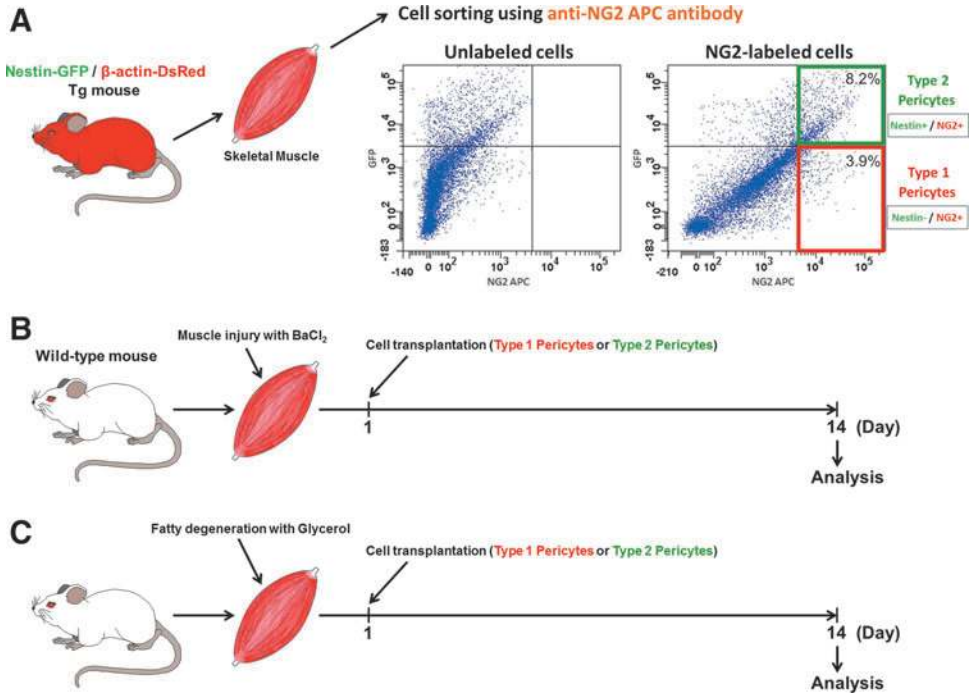

FIG. 6. Diagram of transplantation procedures used to track the fate of type-1 and type-2 pericytes in vivo. **(A)** Obtaining single cells from Nestin-GFP/β-actin-DsRed double-transgenic mouse skeletal muscle, in which all cells are DsRed+. Representative dot plots showing GFP fluorescence versus NG2+ cells with the gate set using unlabeled cells. Protocol for cell transplantation in models of injury **(B)** and fatty degeneration **(C)** in skeletal muscle. Color images available online at www.liebertpub.com/scd

muscles of injured wild-type mice. Two freshly isolated pericyte subtypes were transplanted immediately after cell sorting (Fig. 6A, B). After 2 weeks, the few DsRed+ cells observed in the muscles injected with the adipogenic type-1 pericyte were located in the interstitial connective tissue. No newly formed DsRed+ myofibers were detected (Fig. 8). In contrast, transplanted muscles with type-2 pericytes showed numerous regenerating DsRed+ myofibers with central nuclei (Fig. 8). Quantitative analysis revealed that myogenic potential was found exclusively in the Nestin-GFP+/NG2+/β-actin-DsRed+ cell population. Nestin-GFP+/NG2+/β-actin-DsRed+ cells formed 68±9 DsRed+ myofibers per mm^2 (Fig. 8). We did not detect any DsRed+ myofibers in muscles injected with type-1 pericytes, indicating that type-2 but not type-1 are myogenic in vivo. All DsRed+ type-1 pericytes retain their pericyte marker, NG2 proteoglycan, after injection (Fig. 8D).

Discussion

This work is the first to report the presence of two pericyte subpopulations in the skeletal muscle and to characterize their specific roles. Type-2 pericytes participate in muscle regeneration, while type-1 contribute to fat accumulation. We propose that successful muscle regeneration results from a balance of myogenic and nonmyogenic programs in which the differentiation potential of these pericyte subtypes plays a significant role (Fig. 9).

Although stem cells ensure tissue regeneration, overgrowth of adipogenic cells may compromise organ recovery and impair function [63]. In myopathies and muscle atrophy associated with aging (sarcopenia), fat accumulation increases dysfunction [1,2,53,64], and after chronic injury, the process of fatty degeneration, in which muscle is replaced by white adipocytes, compromises tissue function and environment.

Here we describe the two pericyte subtypes we identified and propose that in skeletal muscle, they are committed to distinct lineages.

Pericytes are stem cells

Pericytes are considered relatively undifferentiated connective tissue cells associated with the walls of small blood vessels and supporting other cells [65]. Mesenchymal stem cells (MSCs) with similar characteristics and developmental potentials have been obtained from several organs [66]. Because blood vessels are distributed in almost all organs, cells associated with them are thought to act like MSCs [33,66]. Further, pericytes have been suggested to locate within a MSC niche [67]. Among their diverse functions, they have been shown to act as multipotent stem cells, differentiating along mesenchymal or neuronal lineages, depending on the microenvironment [12,13,16,47,68–94]. We found that pericytes are differentially committed to an adipogenic or myogenic lineage in response to muscle injury, and therefore, they might be multipotent as a population [13], but more lineage restricted at the cellular level.

Pericytes are heterogeneous

Pericytes are heterogeneous in origin, location, and morphology, ranging from circular to elongated fibroblast-like cells [95–99]. Moreover, their molecular marker expression varies along the vasculature and depends on species, organ, type of blood vessel, location, and developmental stage [100–110]. For this reason, we recommend using more than one marker to identify them [111]. In skeletal muscle, capillary pericytes are also heterogeneous [16,112].

Although their functional diversity is still unexplored, different pericyte subtypes may regulate blood flow and other metabolic functions [95,113]. Recently, a pericyte subtype

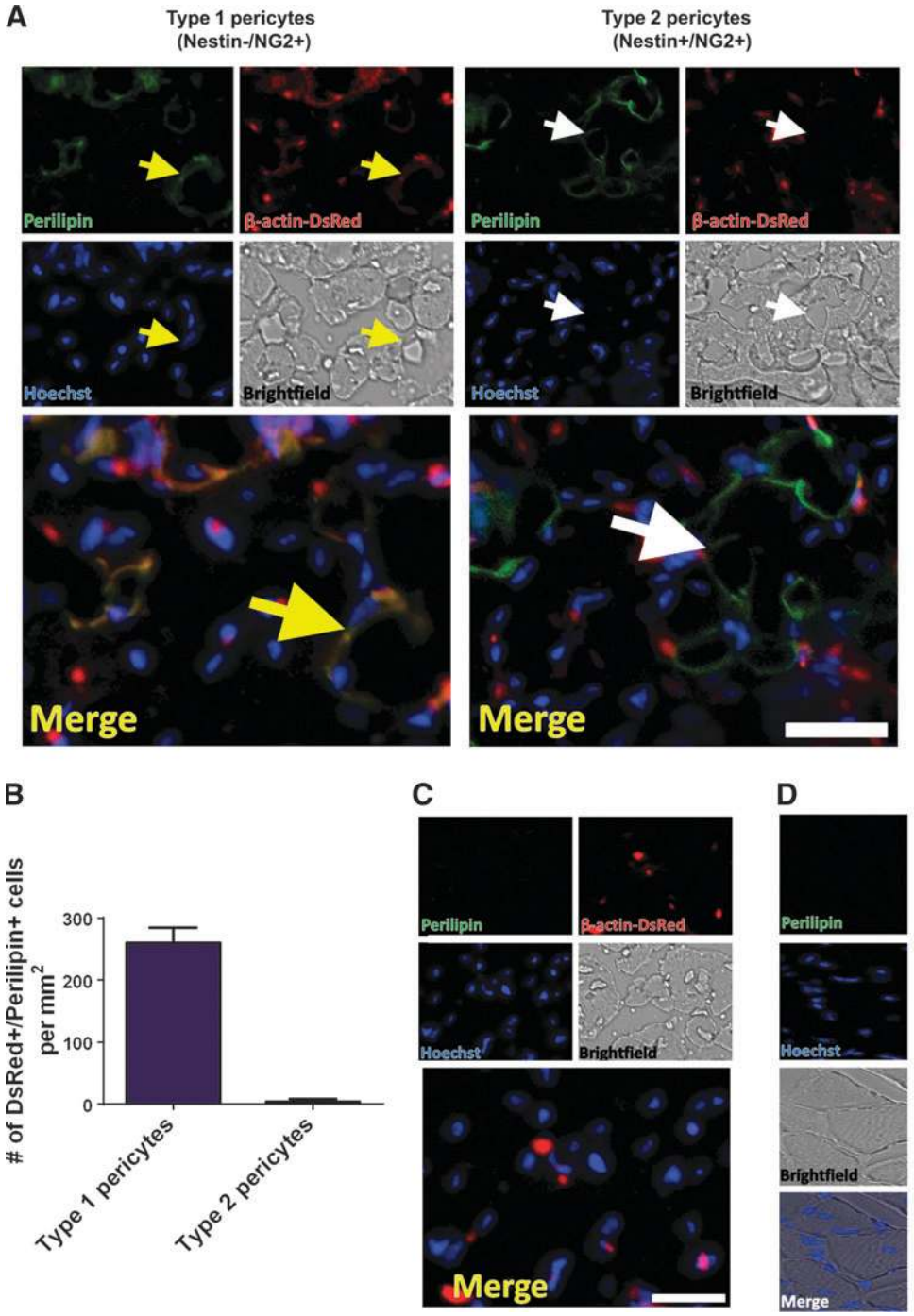

FIG. 7. Type-1 pericyte adipogenic potential in vivo. **(A)** Fourteen days after type-1 or type-2 pericytes were transplanted into glycerol-injured muscle, muscle sections were analyzed for perilipin expression. Representative perilipin expression (*green*), DsRed fluorescence, Hoechst, brightfield, and merge images of the same region. Colocalization of DsRed+ cells with perilipin, shown by the *yellow arrow* in the merged image, supports adipogenic differentiation of transplanted type-1 pericytes. Note that DsRed+ type-2 pericytes do not differentiate into adipocytes (perilipin−) in vivo; all perilipin+ (*green*) adipocytes are DsRed− as indicated by the *white arrow* in the merged image. **(B)** Quantitative analysis of transplantation experiments. Data are mean ± SEM. ($n = 5$ replicates). **(C)** Section of the muscle represented in **(A),** incubated with the fluorescent secondary but not the primary antiperilipin antibody. **(D)** Control section of a regenerated muscle stained with perilipin. Notice that perilipin does not stain myofibers. Scale bars = 50 μm. Color images available online at www.liebertpub.com/scd

was associated with scar formation after spinal cord injury [28]; it may correspond to the type-1 pericytes we describe here and previously in our culture system [16]. Figure 9 demonstrates the heterogeneous role these pericytes play in skeletal muscle healing. We expect this study to elucidate the roles of pericyte subtypes in other tissues.

Adipogenic potential is restricted to type-1 pericytes in skeletal muscle

We found that type-1 but not type-2 pericytes express PDGFRα. Expression of this maker has also been observed in subtypes of mesenchymal progenitor cells, and its activation appears to regulate a broad range of cells in various developmental processes [114]. For example, PDGFRα is initially expressed throughout the undifferentiated somite but disappears in the myotome as differentiation proceeds [115]. In adult skeletal muscle, adipogenic potential was detected only in PDGFRα+ cells [10,25,116], consistent with our finding that only type-1 pericytes, the subtype that expresses this marker, differentiate into adipocytes in skeletal muscle undergoing fatty degeneration. Additionally, skeletal muscle PDGFRα+ cells have been reported to be fibrogenic [10,25,117]. Moreover, only pericytes expressing PDGFRα

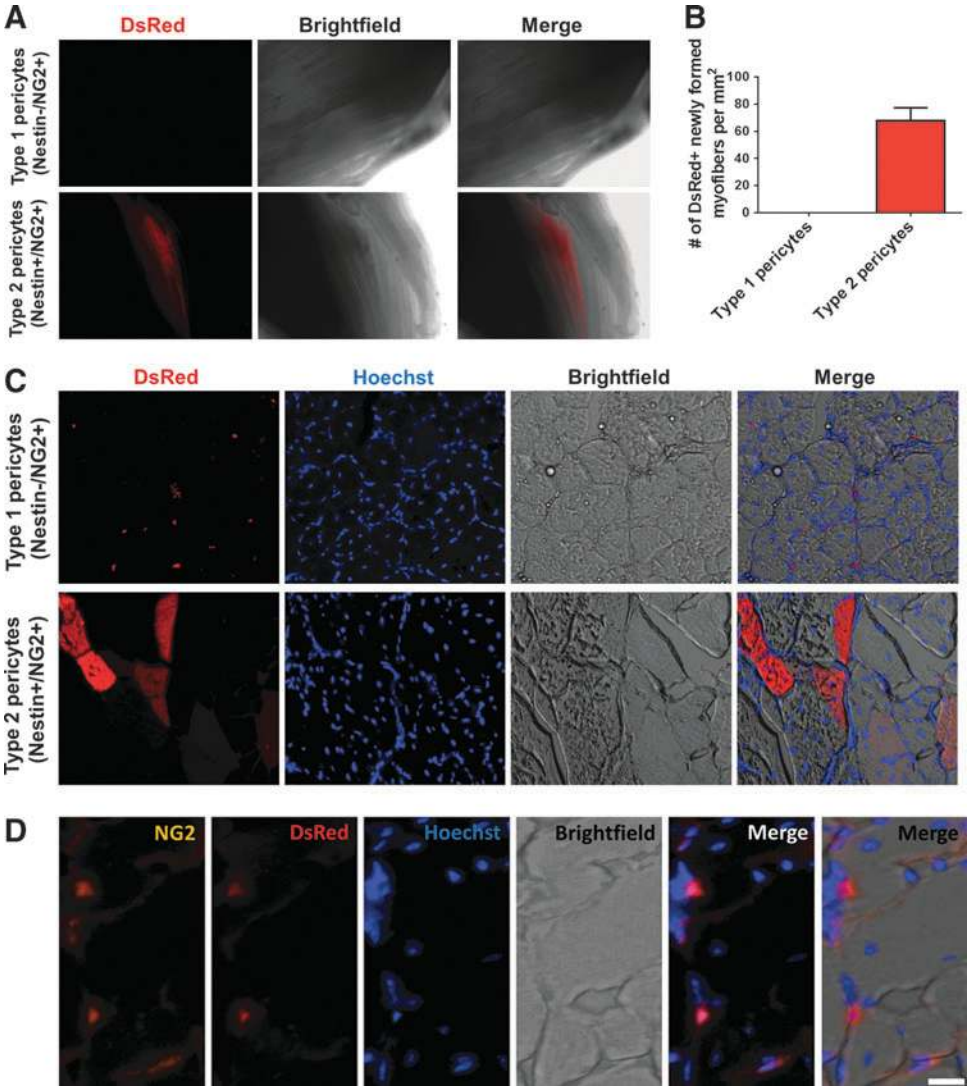

FIG. 8. Only type-2 pericytes generate myofibers after transplantation into injured skeletal muscle. **(A)** DsRed fluorescence in whole TA muscles 2 weeks after injection with type-1 or type-2 pericytes. DsRed+ fibers can be detected only in muscle injected with type-2 pericytes. **(B)** Quantitative analysis of newly formed DsRed+ myofibers with characteristic central nuclei derived from type-1 or type-2 pericytes. Data are mean ± SEM ($n = 5$ replicates). **(C)** At day 14 after transplantation, clusters of DsRed myofibers (*red*) are present throughout the muscle of mice injected with type-2 pericytes. Type-1 pericytes stay in the interstitial space and do not differentiate into muscle cells. **(D)** Representative TA muscle section from a transplanted mouse (as in **C**), showing that type-1 pericytes (DsRed+) retain the expression of the pericyte marker NG2 proteoglycan. Scale bar = 20 μm. Color images available online at www.liebertpub.com/scd

participate in scar formation after spinal cord injury [28], suggesting that they are similar to type-1 pericytes.

Adipogenic pericytes do not form skeletal muscle

More than 30 years ago, studies proposed that pericytes form adipocytes; that is, that an uncommon subset of resident cells located near endothelial cells had long cytoplasmic processes (like pericytes) and acted as a reserve of adipocytes. After activation and migration from the capillary basement membrane, they would differentiate into immature adipocytes with small lipid droplet inclusions [118–121].

More recently, molecular techniques confirmed pericyte differentiation into adipocytes [32]. The emerging biology of MSCs provided indirect support for the possibility that adipogenic progenitors reside near the vasculature [48,87,122,123].

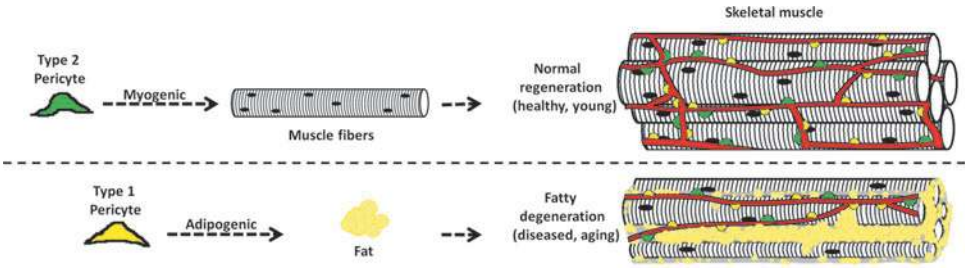

FIG. 9. Schematic representation of normal regenerating and fatty degenerating skeletal muscle. Two pericyte subtypes are associated with blood vessels: type-1 (*yellow*) and type-2 (*green*). We suggest that type-1 pericytes contribute to the adipose infiltration observed in various disorders, such as obesity, dystrophies, and aging, while type-2 pericytes cooperate with myogenesis after healing in normal adult skeletal muscle. Color images available online at www.liebertpub.com/scd

In 2008, adipogenic potential was confirmed in skeletal muscle resident pericytes [13,33,66,124–127]. Pericytes were also shown to form skeletal muscle fibers after muscle injury and in a mouse model of muscular dystrophy [11].

Although adipogenic progenitors isolated from subcutaneous and parametrial white fat depots were shown to fuse with differentiating C2C12 myoblasts in vitro [45], skeletal muscle-derived adipogenic progenitors cannot be recruited to the myogenic lineage even in coculture with myogenic cells [10,25]. These data suggest that myogenic pericytes are distinct from adipogenic pericytes in the skeletal muscle, consistent with the concept that adipogenic pericytes (type-1) are distinct from myogenic pericytes (type-2) and cannot form muscle cells in response to muscle injury.

Muscle cells with myogenic or adipogenic potential

Multiple cell types are present in the skeletal muscle. Satellite cells are thought to be the main source of myoblasts for muscle regeneration in adults [128]; however, their interaction with other cell populations is necessary for efficient muscle formation [52,129]. Other cells show myogenic potential, including muscle side population cells [44,130], PW1+ interstitial cells [131,132], CD133+ mononucleated cells from peripheral blood [133], and myo-endothelial progenitors [134]. Skeletal muscle pericytes have been shown to be multipotent, exhibiting both myogenic and adipogenic potential [13]. However, fibro/adipogenic progenitors have been shown to be the only muscle cells with adipogenic potential [10]; and they do not assume myogenic lineage [10]. Our work shows that a subpopulation of type-1 pericytes included in the fibro/adipogenic progenitor cells (PDGFRα+) exhibits adipogenic potential, while type-2 pericytes are myogenic.

Acknowledgments

The present study was supported by a Wake Forest Pepper Center Pilot Project and PUSH grant from the Wake Forest Comprehensive Cancer Center to Drs. Osvaldo Delbono and Akiva Mintz, grants from the National Institutes of Health/National Institute on Aging (AG13934 and AG15820) to Dr. Osvaldo Delbono, the Wake Forest Claude D. Pepper Older Americans Independence Center (P30-AG21332), and the National Institute of Aging (R01AG040209), National Institute of Mental Health (R01MH092928) and NYSTEM and grant 11.G34.31.0071 from Russian Ministry of Education and Science to Grigori N. Enikolopov. We thank Dr. W. Stallcup from the Sanford-Burnham Medical Research Institute, California, for sharing the rabbit anti-PDGFRα and anti-PDGFRβ antibodies with us and Dr. James Wood for his expert support on flow cytometry of the Comprehensive Cancer Center of WFSM.

Author Disclosure Statement

No competing financial interests exist.

References

1. Goodpaster BH and D Wolf. (2004). Skeletal muscle lipid accumulation in obesity, insulin resistance, and type 2 diabetes. Pediatr Diabetes 5:219–226.
2. Visser M, BH Goodpaster, SB Kritchevsky, AB Newman, M Nevitt, SM Rubin, EM Simonsick and TB Harris. (2005). Muscle mass, muscle strength, and muscle fat infiltration as predictors of incident mobility limitations in well-functioning older persons. J Gerontol A Biol Sci Med Sci 60:324–333.
3. Pahor M and S Kritchevsky. (1998). Research hypotheses on muscle wasting, aging, loss of function and disability. J Nutr Health Aging 2:97–100.
4. Delmonico MJ, TB Harris, M Visser, SW Park, MB Conroy, P Velasquez-Mieyer, R Boudreau, TM Manini, M Nevitt, AB Newman and BH Goodpaster. (2009). Longitudinal study of muscle strength, quality, and adipose tissue infiltration. Am J Clin Nutr 90:1579–1585.
5. Emery AE. (2002). The muscular dystrophies. Lancet 359: 687–695.
6. McNally EM and P Pytel. (2007). Muscle diseases: the muscular dystrophies. Annu Rev Pathol 2:87–109.
7. Wren TA, S Bluml, L Tseng-Ong and V Gilsanz. (2008). Three-point technique of fat quantification of muscle tissue as a marker of disease progression in Duchenne muscular dystrophy: preliminary study. AJR Am J Roentgenol 190: W8–12.
8. Shefer G, M Wleklinski-Lee and Z Yablonka-Reuveni. (2004). Skeletal muscle satellite cells can spontaneously enter an alternative mesenchymal pathway. J Cell Sci 117: 5393–5404.
9. Starkey JD, M Yamamoto, S Yamamoto and DJ Goldhamer. (2011). Skeletal muscle satellite cells are committed to myogenesis and do not spontaneously adopt nonmyogenic fates. J Histochem Cytochem 59:33–46.
10. Uezumi A, S Fukada, N Yamamoto, S Takeda and K Tsuchida. (2010). Mesenchymal progenitors distinct from satellite cells contribute to ectopic fat cell formation in skeletal muscle. Nat Cell Biol 12:143–152.
11. Dellavalle A, G Maroli, D Covarello, E Azzoni, A Innocenzi, L Perani, S Antonini, R Sambasivan, S Brunelli, S Tajbakhsh and G Cossu. (2011). Pericytes resident in postnatal skeletal muscle differentiate into muscle fibres and generate satellite cells. Nat Commun 2:499.
12. Dellavalle A, M Sampaolesi, R Tonlorenzi, E Tagliafico, B Sacchetti, L Perani, A Innocenzi, BG Galvez, G Messina, et al. (2007). Pericytes of human skeletal muscle are myogenic precursors distinct from satellite cells. Nat Cell Biol 9: 255–267.
13. Crisan M, S Yap, L Casteilla, CW Chen, M Corselli, TS Park, G Andriolo, B Sun, B Zheng, et al. (2008). A perivascular origin for mesenchymal stem cells in multiple human organs. Cell Stem Cell 3:301–313.
14. Birbrair A, ZM Wang, ML Messi, GN Enikolopov and O Delbono. (2011). Nestin-GFP transgene reveals neural precursor cells in adult skeletal muscle. PLoS One 6:e16816.
15. Birbrair A, T Zhang, ZM Wang, ML Messi, GN Enikolopov, A Mintz and O Delbono. (2013). Skeletal muscle neural progenitor cells exhibit properties of NG2-glia. Exp Cell Res 319:45–63.
16. Birbrair A, T Zhang, ZM Wang, ML Messi, GN Enikolopov, A Mintz and O Delbono. (2013). Skeletal muscle pericyte subtypes differ in their differentiation potential. Stem Cell Res 10:67–84.
17. Mignone JL, V Kukekov, AS Chiang, D Steindler and G Enikolopov. (2004). Neural stem and progenitor cells in nestin-GFP transgenic mice. J Comp Neurol 469:311–324.

18. Zhu X, DE Bergles and A Nishiyama. (2008). NG2 cells generate both oligodendrocytes and gray matter astrocytes. Development 135:145–157.
19. Vintersten K, C Monetti, M Gertsenstein, P Zhang, L Laszlo, S Biechele and A Nagy. (2004). Mouse in red: red fluorescent protein expression in mouse ES cells, embryos, and adult animals. Genesis 40:241–246.
20. Fink T and V Zachar. (2011). Adipogenic differentiation of human mesenchymal stem cells. Methods Mol Biol 698: 243–251.
21. Zhang T, A Birbrair, ZM Wang, J Taylor, ML Messi and O Delbono. (2011). Troponin T nuclear localization and its role in aging skeletal muscle. Age (Dordr) 35:353–370.
22. Zhang T, A Birbrair and O Delbono. (2013). Nonmyofilament-associated troponin T3 nuclear and nucleolar localization sequence and leucine zipper domain mediate muscle cell apoptosis. Cytoskeleton (Hoboken) 70:134–147.
23. Ge Y, AL Wu, C Warnes, J Liu, C Zhang, H Kawasome, N Terada, MD Boppart, CJ Schoenherr and J Chen. (2009). mTOR regulates skeletal muscle regeneration *in vivo* through kinase-dependent and kinase-independent mechanisms. Am J Physiol Cell Physiol 297:C1434–1444.
24. Ge Y, Y Sun and J Chen. (2011). IGF-II is regulated by microRNA-125b in skeletal myogenesis. J Cell Biol 192: 69–81.
25. Joe AW, L Yi, A Natarajan, F Le Grand, L So, J Wang, MA Rudnicki and FM Rossi. (2010). Muscle injury activates resident fibro/adipogenic progenitors that facilitate myogenesis. Nat Cell Biol 12:153–163.
26. Pisani DF, CD Bottema, C Butori, C Dani and CA Dechesne. (2010). Mouse model of skeletal muscle adiposity: a glycerol treatment approach. Biochem Biophys Res Commun 396:767–773.
27. Greenberg AS, JJ Egan, SA Wek, NB Garty, EJ Blanchette-Mackie and C Londos. (1991). Perilipin, a major hormonally regulated adipocyte-specific phosphoprotein associated with the periphery of lipid storage droplets. J Biol Chem 266: 11341–11346.
28. Goritz C, DO Dias, N Tomilin, M Barbacid, O Shupliakov and J Frisen. (2011). A pericyte origin of spinal cord scar tissue. Science 333:238–242.
29. Fleming JN, RA Nash, DO McLeod, DF Fiorentino, HM Shulman, MK Connolly, JA Molitor, G Henstorf, R Lafyatis, et al. (2008). Capillary regeneration in scleroderma: stem cell therapy reverses phenotype? PLoS One 3:e1452.
30. Hellstrom M, M Kalen, P Lindahl, A Abramsson and C Betsholtz. (1999). Role of PDGF-B and PDGFR-beta in recruitment of vascular smooth muscle cells and pericytes during embryonic blood vessel formation in the mouse. Development 126:3047–3055.
31. Sacchetti B, A Funari, S Michienzi, S Di Cesare, S Piersanti, I Saggio, E Tagliafico, S Ferrari, PG Robey, M Riminucci and P Bianco. (2007). Self-renewing osteoprogenitors in bone marrow sinusoids can organize a hematopoietic microenvironment. Cell 131:324–336.
32. Farrington-Rock C, NJ Crofts, MJ Doherty, BA Ashton, C Griffin-Jones and AE Canfield. (2004). Chondrogenic and adipogenic potential of microvascular pericytes. Circulation 110:2226–2232.
33. Caplan AI. (2008). All MSCs are pericytes? Cell Stem Cell 3:229–230.
34. Ba K, X Yang, L Wu, X Wei, N Fu, Y Fu, X Cai, Y Yao, Y Ge and Y Lin. (2012). Jagged-1-mediated activation of notch signalling induces adipogenesis of adipose-derived stem cells. Cell Prolif 45:538–544.
35. Wright WE, DA Sassoon and VK Lin. (1989). Myogenin, a factor regulating myogenesis, has a domain homologous to MyoD. Cell 56:607–617.
36. Parlakian A, I Gomaa, S Solly, L Arandel, A Mahale, G Born, G Marazzi and D Sassoon. (2010). Skeletal muscle phenotypically converts and selectively inhibits metastatic cells in mice. PLoS One 5:e9299.
37. Mauro A. (1961). Satellite cell of skeletal muscle fibers. J Biophys Biochem Cytol 9:493–495.
38. Day K, G Shefer, JB Richardson, G Enikolopov and Z Yablonka-Reuveni. (2007). Nestin-GFP reporter expression defines the quiescent state of skeletal muscle satellite cells. Dev Biol 304:246–259.
39. Seale P, LA Sabourin, A Girgis-Gabardo, A Mansouri, P Gruss and MA Rudnicki. (2000). Pax7 is required for the specification of myogenic satellite cells. Cell 102: 777–786.
40. Relaix F, D Montarras, S Zaffran, B Gayraud-Morel, D Rocancourt, S Tajbakhsh, A Mansouri, A Cumano and M Buckingham. (2006). Pax3 and Pax7 have distinct and overlapping functions in adult muscle progenitor cells. J Cell Biol 172:91–102.
41. Oustanina S, G Hause and T Braun. (2004). Pax7 directs postnatal renewal and propagation of myogenic satellite cells but not their specification. EMBO J 23:3430–3439.
42. Kuang S, SB Charge, P Seale, M Huh and MA Rudnicki. (2006). Distinct roles for Pax7 and Pax3 in adult regenerative myogenesis. J Cell Biol 172:103–113.
43. Beauchamp JR, L Heslop, DS Yu, S Tajbakhsh, RG Kelly, A Wernig, ME Buckingham, TA Partridge and PS Zammit. (2000). Expression of CD34 and Myf5 defines the majority of quiescent adult skeletal muscle satellite cells. J Cell Biol 151:1221–1234.
44. Asakura A, P Seale, A Girgis-Gabardo and MA Rudnicki. (2002). Myogenic specification of side population cells in skeletal muscle. J Cell Biol 159:123–134.
45. Rodeheffer MS, K Birsoy and JM Friedman. (2008). Identification of white adipocyte progenitor cells *in vivo*. Cell 135:240–249.
46. Zimmerlin L, VS Donnenberg, JP Rubin and AD Donnenberg. (2013). Mesenchymal markers on human adipose stem/progenitor cells. Cytometry A 83:134–140.
47. Zimmerlin L, VS Donnenberg and AD Donnenberg. (2011). Rare event detection and analysis in flow cytometry: bone marrow mesenchymal stem cells, breast cancer stem/progenitor cells in malignant effusions, and pericytes in disaggregated adipose tissue. Methods Mol Biol 699:251–273.
48. Traktuev DO, S Merfeld-Clauss, J Li, M Kolonin, W Arap, R Pasqualini, BH Johnstone and KL March. (2008). A population of multipotent CD34-positive adipose stromal cells share pericyte and mesenchymal surface markers, reside in a periendothelial location, and stabilize endothelial networks. Circ Res 102:77–85.
49. Tigges U, M Komatsu and WB Stallcup. (2012). Adventitial pericyte progenitor/mesenchymal stem cells participate in the restenotic response to arterial injury. J Vasc Res 50:134–144.
50. Hall AP. (2006). Review of the pericyte during angiogenesis and its role in cancer and diabetic retinopathy. Toxicol Pathol 34:763–775.

51. Lepper C, TA Partridge and CM Fan. (2011). An absolute requirement for Pax7-positive satellite cells in acute injury-induced skeletal muscle regeneration. Development 138: 3639–3646.
52. Murphy MM, JA Lawson, SJ Mathew, DA Hutcheson and G Kardon. (2011). Satellite cells, connective tissue fibroblasts and their interactions are crucial for muscle regeneration. Development 138:3625–3637.
53. Wallace GQ and EM McNally. (2009). Mechanisms of muscle degeneration, regeneration, and repair in the muscular dystrophies. Annu Rev Physiol 71:37–57.
54. Kawai H, H Nishino, K Kusaka, T Naruo, Y Tamaki and M Iwasa. (1990). Experimental glycerol myopathy: a histological study. Acta Neuropathol 80:192–197.
55. Pisani DF, N Clement, A Loubat, M Plaisant, S Sacconi, JY Kurzenne, C Desnuelle, C Dani and CA Dechesne. (2010). Hierarchization of myogenic and adipogenic progenitors within human skeletal muscle. Stem Cells 28:2182–2194.
56. Abraham ST and C Shaw. (2006). Increased expression of deltaCaMKII isoforms in skeletal muscle regeneration: implications in dystrophic muscle disease. J Cell Biochem 97:621–632.
57. Yen YP, KS Tsai, YW Chen, CF Huang, RS Yang and SH Liu. (2010). Arsenic inhibits myogenic differentiation and muscle regeneration. Environ Health Perspect 118:949–956.
58. Pisani DF, CA Dechesne, S Sacconi, S Delplace, N Belmonte, O Cochet, N Clement, B Wdziekonski, AP Villageois, et al. (2010). Isolation of a highly myogenic CD34-negative subset of human skeletal muscle cells free of adipogenic potential. Stem Cells 28:753–764.
59. Suelves M, R Lopez-Alemany, F Lluis, G Aniorte, E Serrano, M Parra, P Carmeliet and P Munoz-Canoves. (2002). Plasmin activity is required for myogenesis *in vitro* and skeletal muscle regeneration *in vivo*. Blood 99:2835–2844.
60. Lluis F, J Roma, M Suelves, M Parra, G Aniorte, E Gallardo, I Illa, L Rodriguez, SM Hughes, et al. (2001). Urokinase-dependent plasminogen activation is required for efficient skeletal muscle regeneration *in vivo*. Blood 97:1703–1711.
61. Arsic N, S Zacchigna, L Zentilin, G Ramirez-Correa, L Pattarini, A Salvi, G Sinagra and M Giacca. (2004). Vascular endothelial growth factor stimulates skeletal muscle regeneration *in vivo*. Mol Ther 10:844–854.
62. Caldwell CJ, DL Mattey and RO Weller. (1990). Role of the basement membrane in the regeneration of skeletal muscle. Neuropathol Appl Neurobiol 16:225–238.
63. Wynn TA. (2008). Cellular and molecular mechanisms of fibrosis. J Pathol 214:199–210.
64. Masgrau A, A Mishellany-Dutour, H Murakami, AM Beaufrere, S Walrand, C Giraudet, C Migne, M Gerbaix, L Metz, et al. (2012). Time-course changes of muscle protein synthesis associated with obesity-induced lipotoxicity. J Physiol 590:5199–5210.
65. Bonkowski D, V Katyshev, RD Balabanov, A Borisov and P Dore-Duffy. (2011). The CNS microvascular pericyte: pericyte-astrocyte crosstalk in the regulation of tissue survival. Fluids Barriers CNS 8:8.
66. Corselli M, CW Chen, M Crisan, L Lazzari and B Peault. (2010). Perivascular ancestors of adult multipotent stem cells. Arterioscler Thromb Vasc Biol 30:1104–1109.
67. Feng J, A Mantesso and PT Sharpe. (2010). Perivascular cells as mesenchymal stem cells. Expert Opin Biol Ther 10: 1441–1451.
68. Canfield AE, AB Sutton, JA Hoyland and AM Schor. (1996). Association of thrombospondin-1 with osteogenic differentiation of retinal pericytes *in vitro*. J Cell Sci 109 (Pt 2):343–353.
69. Doherty MJ, BA Ashton, S Walsh, JN Beresford, ME Grant and AE Canfield. (1998). Vascular pericytes express osteogenic potential *in vitro* and *in vivo*. J Bone Miner Res 13: 828–838.
70. Dore-Duffy P, A Katychev, X Wang and E Van Buren. (2006). CNS microvascular pericytes exhibit multipotential stem cell activity. J Cereb Blood Flow Metab 26:613–624.
71. Karow M, R Sanchez, C Schichor, G Masserdotti, F Ortega, C Heinrich, S Gascon, MA Khan, DC Lie, et al. (2012). Reprogramming of pericyte-derived cells of the adult human brain into induced neuronal cells. Cell Stem Cell 11:471–476.
72. Diaz-Manera J, E Gallardo, N de Luna, M Navas, L Soria, M Garibaldi, R Rojas-Garcia, R Tonlorenzi, G Cossu and I Illa. (2012). The increase of pericyte population in human neuromuscular disorders supports their role in muscle regeneration *in vivo*. J Pathol 228:544–555.
73. Chunmeng S and C Tianmin. (2004). Skin: a promising reservoir for adult stem cell populations. Med Hypotheses 62:683–688.
74. Herrera MB, S Bruno, S Buttiglieri, C Tetta, S Gatti, MC Deregibus, B Bussolati and G Camussi. (2006). Isolation and characterization of a stem cell population from adult human liver. Stem Cells 24:2840–2850.
75. Saif J, C Heeschen and A Aicher. (2009). Add some fat to vascular progenitor cell therapy. Circ Res 104:1330–1332.
76. Lin CS, ZC Xin, CH Deng, H Ning, G Lin and TF Lue. (2010). Defining adipose tissue-derived stem cells in tissue and in culture. Histol Histopathol 25:807–815.
77. Humphreys BD, SL Lin, A Kobayashi, TE Hudson, BT Nowlin, JV Bonventre, MT Valerius, AP McMahon and JS Duffield. (2010). Fate tracing reveals the pericyte and not epithelial origin of myofibroblasts in kidney fibrosis. Am J Pathol 176:85–97.
78. Paquet-Fifield S, RP Redvers, N Pouliot and P Kaur. (2010). A transplant model for human epidermal skin regeneration. Methods Mol Biol 585:369–382.
79. Cai X, Y Lin, CC Friedrich, C Neville, I Pomerantseva, CA Sundback, Z Zhang, JP Vacanti, PV Hauschka and BE Grottkau. (2009). Bone marrow derived pluripotent cells are pericytes which contribute to vascularization. Stem Cell Rev 5:437–445.
80. Klein D, HP Hohn, V Kleff, D Tilki and S Ergun. (2010). Vascular wall-resident stem cells. Histol Histopathol 25: 681–689.
81. Ergun S, D Tilki and D Klein. (2011). Vascular wall as a reservoir for different types of stem and progenitor cells. Antioxid Redox Signal 15:981–995.
82. Nehls V and D Drenckhahn. (1993). The versatility of microvascular pericytes: from mesenchyme to smooth muscle? Histochemistry 99:1–12.
83. Satokata I, L Ma, H Ohshima, M Bei, I Woo, K Nishizawa, T Maeda, Y Takano, M Uchiyama, et al. (2000). Msx2 deficiency in mice causes pleiotropic defects in bone growth and ectodermal organ formation. Nat Genet 24:391–395.
84. Alliot-Licht B, D Hurtrel and M Gregoire. (2001). Characterization of alpha-smooth muscle actin positive cells in mineralized human dental pulp cultures. Arch Oral Biol 46:221–228.
85. Shi S and S Gronthos. (2003). Perivascular niche of postnatal mesenchymal stem cells in human bone marrow and dental pulp. J Bone Miner Res 18:696–704.

86. da Silva Meirelles L, AI Caplan and NB Nardi. (2008). In search of the *in vivo* identity of mesenchymal stem cells. Stem Cells 26:2287–2299.
87. Lin G, M Garcia, H Ning, L Banie, YL Guo, TF Lue and CS Lin. (2008). Defining stem and progenitor cells within adipose tissue. Stem Cells Dev 17:1053–1063.
88. Caplan AI. (2007). Adult mesenchymal stem cells for tissue engineering versus regenerative medicine. J Cell Physiol 213:341–347.
89. Dore-Duffy P, A Mehedi, X Wang, M Bradley, R Trotter and A Gow. (2011). Immortalized CNS pericytes are quiescent smooth muscle actin-negative and pluripotent. Microvasc Res 82:18–27.
90. Maier CL, BR Shepherd, T Yi and JS Pober. (2010). Explant outgrowth, propagation and characterization of human pericytes. Microcirculation 17:367–380.
91. Feng J, A Mantesso, C De Bari, A Nishiyama and PT Sharpe. (2011). Dual origin of mesenchymal stem cells contributing to organ growth and repair. Proc Natl Acad Sci U S A 108:6503–6508.
92. Jung KH, K Chu, ST Lee, JJ Bahn, D Jeon, JH Kim, S Kim, CH Won, M Kim, SK Lee and JK Roh. (2011). Multipotent PDGFRbeta-expressing cells in the circulation of stroke patients. Neurobiol Dis 41:489–497.
93. Dore-Duffy P. (2008). Pericytes: pluripotent cells of the blood brain barrier. Curr Pharm Des 14:1581–1593.
94. Nakagomi T, Z Molnar, A Nakano-Doi, A Taguchi, O Saino, S Kubo, M Clausen, H Yoshikawa, N Nakagomi and T Matsuyama. (2011). Ischemia-induced neural stem/progenitor cells in the pia mater following cortical infarction. Stem Cells Dev 20:2037–2051.
95. Zimmermann KW. (1923). Der feinere Bau der Blutkapillaren. Z Anat Entwicklungsgesch 68:29–109.
96. Shepro D and NM Morel. (1993). Pericyte physiology. FASEB J 7:1031–1038.
97. Sims DE. (1991). Recent advances in pericyte biology—implications for health and disease. Can J Cardiol 7:431–443.
98. Sims DE. (2000). Diversity within pericytes. Clin Exp Pharmacol Physiol 27:842–846.
99. Etchevers HC, C Vincent, NM Le Douarin and GF Couly. (2001). The cephalic neural crest provides pericytes and smooth muscle cells to all blood vessels of the face and forebrain. Development 128:1059–1068.
100. Allt G and JG Lawrenson. (2001). Pericytes: cell biology and pathology. Cells Tissues Organs 169:1–11.
101. Stallcup WB. (2002). The NG2 proteoglycan: past insights and future prospects. J Neurocytol 31:423–435.
102. Ozerdem U and WB Stallcup. (2003). Early contribution of pericytes to angiogenic sprouting and tube formation. Angiogenesis 6:241–249.
103. Hughes S and T Chan-Ling. (2004). Characterization of smooth muscle cell and pericyte differentiation in the rat retina *in vivo*. Invest Ophthalmol Vis Sci 45:2795–2806.
104. Armulik A, A Abramsson and C Betsholtz. (2005). Endothelial/pericyte interactions. Circ Res 97:512–523.
105. Baluk P, H Hashizume and DM McDonald. (2005). Cellular abnormalities of blood vessels as targets in cancer. Curr Opin Genet Dev 15:102–111.
106. Bergers G and S Song. (2005). The role of pericytes in blood-vessel formation and maintenance. Neuro Oncol 7:452–464.
107. Song S, AJ Ewald, W Stallcup, Z Werb and G Bergers. (2005). PDGFRbeta+ perivascular progenitor cells in tumours regulate pericyte differentiation and vascular survival. Nat Cell Biol 7:870–879.
108. Bondjers C, L He, M Takemoto, J Norlin, N Asker, M Hellstrom, P Lindahl and C Betsholtz. (2006). Microarray analysis of blood microvessels from PDGF-B and PDGF-Rbeta mutant mice identifies novel markers for brain pericytes. FASEB J 20:1703–1705.
109. Lamagna C and G Bergers. (2006). The bone marrow constitutes a reservoir of pericyte progenitors. J Leukoc Biol 80:677–681.
110. Murfee WL, MR Rehorn, SM Peirce and TC Skalak. (2006). Perivascular cells along venules upregulate NG2 expression during microvascular remodeling. Microcirculation 13:261–273.
111. Armulik A, G Genove and C Betsholtz. (2011). Pericytes: developmental, physiological, and pathological perspectives, problems, and promises. Dev Cell 21:193–215.
112. Sims D, MM Horne, M Creighan and A Donald. (1994). Heterogeneity of pericyte populations in equine skeletal muscle and dermal microvessels: a quantitative study. Anat Histol Embryol 23:232–238.
113. Nehls V and D Drenckhahn. (1991). Heterogeneity of microvascular pericytes for smooth muscle type alpha-actin. J Cell Biol 113:147–154.
114. Andrae J, R Gallini and C Betsholtz. (2008). Role of platelet-derived growth factors in physiology and medicine. Genes Dev 22:1276–1312.
115. Orr-Urtreger A and P Lonai. (1992). Platelet-derived growth factor-A and its receptor are expressed in separate, but adjacent cell layers of the mouse embryo. Development 115:1045–1058.
116. Rodeheffer MS. (2010). Tipping the scale: muscle versus fat. Nat Cell Biol 12:102–104.
117. Uezumi A, T Ito, D Morikawa, N Shimizu, T Yoneda, M Segawa, M Yamaguchi, R Ogawa, MM Matev, et al. (2011). Fibrosis and adipogenesis originate from a common mesenchymal progenitor in skeletal muscle. J Cell Sci 124: 3654–3664.
118. Hausman GJ, DR Campion and RJ Martin. (1980). Search for the adipocyte precursor cell and factors that promote its differentiation. J Lipid Res 21:657–670.
119. Iyama K, K Ohzono and G Usuku. (1979). Electron microscopical studies on the genesis of white adipocytes: differentiation of immature pericytes into adipocytes in transplanted preadipose tissue. Virchows Arch B Cell Pathol Incl Mol Pathol 31:143–155.
120. Napolitano L. (1963). The differentiation of white adipose cells. An electron microscope study. J Cell Biol 18:663–679.
121. Richardson RL, GJ Hausman and DR Campion. (1982). Response of pericytes to thermal lesion in the inguinal fat pad of 10-day-old rats. Acta Anat (Basel) 114:41–57.
122. Tang W, D Zeve, JM Suh, D Bosnakovski, M Kyba, RE Hammer, MD Tallquist and JM Graff. (2008). White fat progenitor cells reside in the adipose vasculature. Science 322:583–586.
123. Cai X, Y Lin, PV Hauschka and BE Grottkau. (2011). Adipose stem cells originate from perivascular cells. Biol Cell 103:435–447.
124. Crisan M, M Corselli, WC Chen and B Peault. (2012). Perivascular cells for regenerative medicine. J Cell Mol Med 16:2851–2860.
125. Crisan M, M Corselli, CW Chen and B Peault. (2011). Multilineage stem cells in the adult: a perivascular legacy? Organogenesis 7:101–104.
126. Chen CW, E Montelatici, M Crisan, M Corselli, J Huard, L Lazzari and B Peault. (2009). Perivascular multi-lineage

progenitor cells in human organs: regenerative units, cytokine sources or both? Cytokine Growth Factor Rev 20:429–434.
127. Crisan M, CW Chen, M Corselli, G Andriolo, L Lazzari and B Peault. (2009). Perivascular multipotent progenitor cells in human organs. Ann N Y Acad Sci 1176:118–123.
128. Zammit PS. (2008). All muscle satellite cells are equal, but are some more equal than others? J Cell Sci 121:2975–2982.
129. Christov C, F Chretien, R Abou-Khalil, G Bassez, G Vallet, FJ Authier, Y Bassaglia, V Shinin, S Tajbakhsh, B Chazaud and RK Gherardi. (2007). Muscle satellite cells and endothelial cells: close neighbors and privileged partners. Mol Biol Cell 18:1397–1409.
130. Seale P, J Ishibashi, A Scime and MA Rudnicki. (2004). Pax7 is necessary and sufficient for the myogenic specification of CD45+:Sca1+ stem cells from injured muscle. PLoS Biol 2:E130.
131. Mitchell KJ, A Pannerec, B Cadot, A Parlakian, V Besson, ER Gomes, G Marazzi and DA Sassoon. (2010). Identification and characterization of a non-satellite cell muscle resident progenitor during postnatal development. Nat Cell Biol 12:257–266.
132. Nicolas N, G Marazzi, K Kelley and D Sassoon. (2005). Embryonic deregulation of muscle stress signaling pathways leads to altered postnatal stem cell behavior and a failure in postnatal muscle growth. Dev Biol 281:171–183.
133. Torrente Y, M Belicchi, M Sampaolesi, F Pisati, M Meregalli, G D'Antona, R Tonlorenzi, L Porretti, M Gavina, et al. (2004). Human circulating AC133(+) stem cells restore dystrophin expression and ameliorate function in dystrophic skeletal muscle. J Clin Invest 114:182–195.
134. Tamaki T, A Akatsuka, K Ando, Y Nakamura, H Matsuzawa, T Hotta, RR Roy and VR Edgerton. (2002). Identification of myogenic-endothelial progenitor cells in the interstitial spaces of skeletal muscle. J Cell Biol 157:571–577.

Address correspondence to:
Dr. Osvaldo Delbono
Wake Forest School of Medicine
1 Medical Center Boulevard
Winston-Salem, NC 27157

E-mail: odelbono@wakehealth.edu

Received for publication November 17, 2012
Accepted after revision March 20, 2013
Prepublished on Liebert Instant Online March 21, 2013